

Research Journal of Pharmaceutical, Biological and Chemical Sciences

Synthesis and Characterization of Sr-doped $\text{LaFe}_{0.7}\text{Ni}_{0.3}\text{O}_3$ perovskite.

Omar Ben Mya^{1,2*}, and Mahmoud Omari².

¹University of Mohammed Lakhdar Amara, Sciences and techniques department, 39000 El Oued, Algeria.

²University of Mohammed Khider, Matter sciences department, 07000 Biskra, Algeria.

ABSTRACT

$\text{La}_{1-x}\text{Sr}_x\text{Fe}_{0.7}\text{Ni}_{0.3}\text{O}_3$ perovskite nanoparticles, denoted as LSFNx ($x = 0.0, 0.1 \& 0.2$) were prepared using sol-gel combustion method. The effect of Sr- substitution on the structure and thermal treatment is investigated. The XRD patterns of these catalysts indicated that a well-crystallized perovskite structure was formed when LFN and LSFN were calcined at 700°C for 5 h and crystallites sizes are 43.31; 31.5 and 30.8 nm for LFN, LSFN_{0.1} and LSFN_{0.2}, respectively. TEM images show a good agreement with this result. Surface areas evaluated using BET technique shows an important surface area of each sample. XPS technique shows oxidation state of all elements in A and B site, and improve that Ni is the active element. A comparison between samples of this material as electrodes for symmetrical SOFCs by evaluation of Area specific resistances prove that $\text{LFN} < \text{LSFN}_{0.1} < \text{LSFN}_{0.2}$ in efficiency.

Keywords: LSFN, Perovskite, Nanoparticles, specific area resistance, combustion method.

**Corresponding author*

INTRODUCTION

Techniques of use and development of advanced solid oxide fuel cells (SOFC'S) have seen remarkable development, in recent years, because it is clean and renewable source of electric power, and as is well known, access to high technology and high-yield at the lowest cost remains the great challenge in front of materials scientists, Use of perovskite oxides as electrodes or electrolyte in this kind of cells has been investigated in several studies because they have many industrial applications such as thermoelectric power conversion, cathode material for solid oxide fuel cells (SOFCs), steam reforming, oxygen permeable membranes, gas sensors and combustion of hydrocarbons [1-7].

Among of the recent applications of these materials is symmetrical cells that can be cathode and anode at the same time, adoption of this technology and getting best conditions for its application is an achievement in itself in terms of reducing the cost of obtaining high-yield with cheap and available reactants, simple synthesis methods and high thermal stability [8-10].

It is known that perovskite oxides including $\text{LaFe}_{0.7}\text{Ni}_{0.3}\text{O}_3$ can be prepared by several methods such as the Pichini method [11], sol-gel combustion method [12]. It is confirmed that this composition has a best catalytic performance [13]. However, most reports, studied the perovskite structure, have examined the effect of A site doping, which is typically accompanied with strong lattice strain effects. Thus, a thermodynamic study of $\text{La}_{1-x}\text{Sr}_x\text{FeO}_3$ [14] proposed that the doping of the trivalent A site (La^{3+} ions) with divalent ions that have a different valance state, such Sr^{2+} produced the oxygen vacancies and ion conductivity [15]. Also several studies proposed this oxides because of their excellent electrical conductivity (ionic and electronic), catalytic activity to produce oxygen ions, thermal and chemical stability [16-23]. In opposing, the B site is doping by transition metal oxides, nickel substitution in LaFeO_3 results in an increased catalytic performance for combustion of acetyl acetate [2], oxygen permeability [3], electrical conductivity and thermal expansion close to yttria-stabilized zirconia (YSZ) [20], $\text{LaFe}_{1-x}\text{Ni}_x\text{O}_3$ as a potential candidate material is recommended [24] for cathodes in SOFCs in case of pure or doped simultaneously with Sr on A site and Ni (transition metal) on B site due to their mixed ionic and electronic conductivity [19].

The aim of this present work is to study the A-site substitution of Sr in $\text{LaFe}_{0.7}\text{Ni}_{0.3}\text{O}_3$ on electrochemical properties as symmetrical cell in SOFC

EXPERIMENTAL

Synthesis

$\text{La}_{1-x}\text{Sr}_x\text{Fe}_{0.7}\text{Ni}_{0.3}\text{O}_3$, ($x = 0.0, 0.1 \text{ \& } 0.2$) NPs were synthesized by sol-gel combustion method. The starting raw materials used in this work were the Lanthanum nitrate hexahydrate ($\text{La}(\text{NO}_3)_3 \cdot 6\text{H}_2\text{O}$), ferric nitrate nonahydrate $\text{Fe}(\text{NO}_3)_3 \cdot 9\text{H}_2\text{O}$, strontium nitrate ($\text{Sr}(\text{NO}_3)_2$) and nickel nitrate hexahydrate ($\text{Ni}(\text{NO}_3)_2 \cdot 6\text{H}_2\text{O}$) as oxidizing agents, whereas citric acid ($\text{C}_6\text{H}_8\text{O}_7$) was used as fuel. All chemicals completely dissolved in 100 mL diluted water in a beaker under the constant stirrer at 100°C until the homogeneous sol as solution formed.. Afterwards, the homogeneous sol was heated slowly at 120°C for a night. The solid dry gel was calcined at 700°C in air for 5 h. The powders were pressed into pellets and sintered at 1100°C for 1 h.

Powders characterization

The crystal structure and parameters were investigated by x-ray diffraction (diffractometer Bruker D8 Advance) using $\text{Cu-K}\alpha$ radiation ($\lambda = 1.5418 \text{ \AA}$) in 2θ range from 5° to 80° . A Philips CM-200 with 200kv transmission electron microscope was used to check the morphology and particle size. BET technique was used to measure specific area using a Surface Area and Porosity Analyzer, Micrometrics home (ASAP 2020 model). Differential scanning calorimetry and thermo gravimetric analysis (DSC/TGA) data were recorded on a STA 409 PC Lux. The temperature was varied from 10 to 1000°C at a heating/cooling rate of $10^\circ\text{C min}^{-1}$. All spectra were measured using XPS. ESCA 701 from physical electronics (PHI). Collected XPS spectra having ASCII and SPE formats for survey and narrow scans were analyzed using Multipack software. All spectra were calibrated using the adventitious C 1s peak with a fixed value of 284.8 eV .

Area-specific resistance measurements

Area specific polarisation resistance (ASR) values were obtained under symmetrical atmospheres (without chemical potential gradient) in a two electrode configuration. The electrode powders were mixed in a 50 wt.% with Decoflux™ (WB41, Zschimmer and Schwarz) as binder material to obtain a slurry which was used to paint symmetrical electrodes on dense pellets of the LSGM electrolyte. The electrodes were sintered at 1100 °C for 1 h to ensure a good adherence with the electrolyte. Symmetrical cells with a CGO buffer layer between the electrolyte and electrode materials were also investigated in order to prevent a possible reaction between both materials. The CGO buffer was fixed on an as-prepared $\text{La}_{0.9}\text{Sr}_{0.1}\text{OGa}_{0.80}\text{Mg}_{0.20}\text{O}_3$ (LSGM-9182) as the electrolyte show a systematic improvement in the electrode performance. Pt-ink electrodes were used as current collectors.

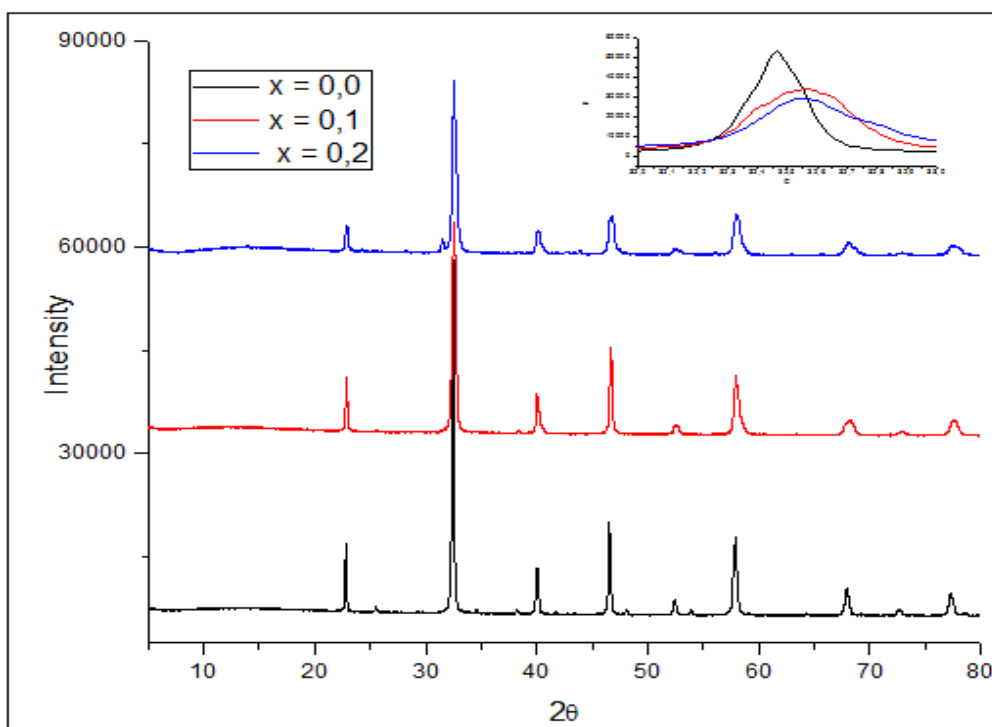
The symmetrical cells were measured by impedance spectroscopy under air using a 1260 Solartron FRA in the 0.1–10⁶ Hz frequency range from 900 to 500 °C with a cooling rate of 5 °C min⁻¹ and a stabilization time of 30 min between measurements. An ac signal of 50 mV was applied to obtain reproducible spectra. The data were analyzed with ZView software [23]

RESULTS & DISCUSSION

Structural Characterization

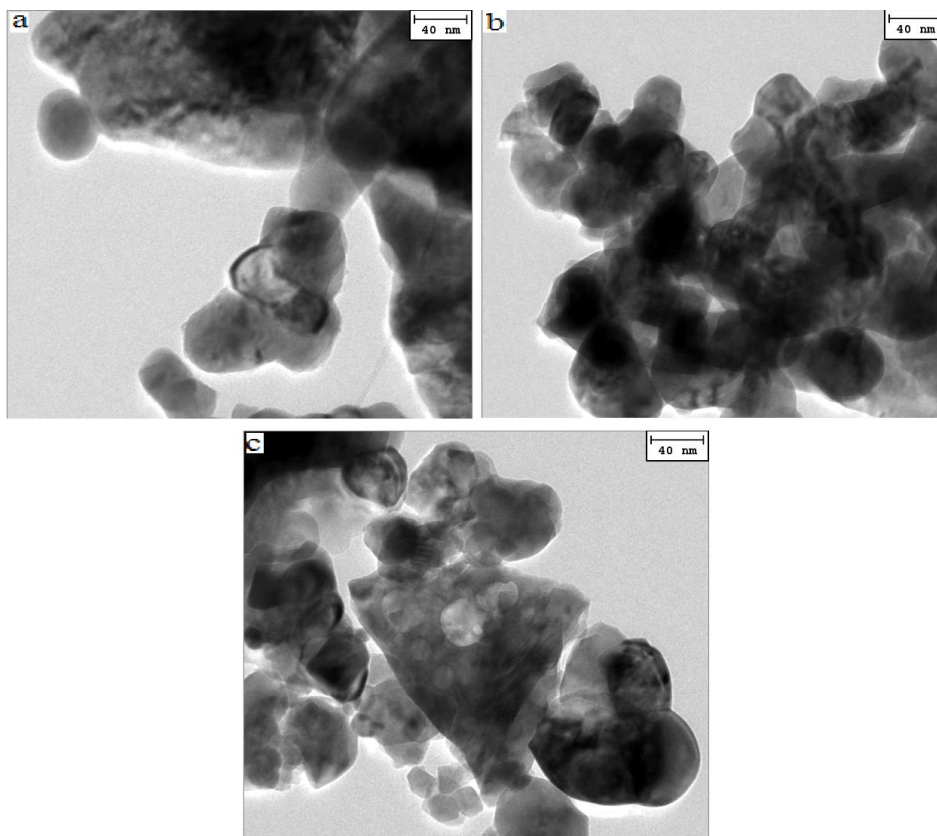
The x-ray diffraction (XRD) patterns of $\text{La}_{1-x}\text{Sr}_x\text{Fe}_{0.7}\text{Ni}_{0.3}\text{O}_3$, ($x = 0.0, 0.1 \text{ \& } 0.2$) nano powders, calcined at 700°C are shown in Fig. 1. The position of the all peaks confirmed the high crystallinity and perovskite structure of the NPs and no other impurity peaks were detected in the XRD patterns, only one small peak in $x = 0.2$ XRD patterns corresponding to LaNiO_3 [25]. Furthermore, the product of the $\text{LSFN}_{0.0}$ sample was observed in orthorhombic perovskite structure with space group Pbnm, which is well consistent with the standard JCPDS card of perovskite $\text{LaFe}_{0.75}\text{Ni}_{0.25}\text{O}_3$ JCPDS37-1493). The lattice parameters slightly decreased with the value of doped Sr, due to the different in ionic radius, resulted small shifting of peaks to higher 2θ values. The average of crystallite size is calculated using the most intense peak [11].

Figure 1: XRD patterns of $\text{La}_{1-x}\text{Sr}_x\text{Fe}_{0.7}\text{Ni}_{0.3}\text{O}_3$ (0.0, 0.1 & 0.2) nanopowders



TEM was employed to obtain direct information about the size and structure of the produced LSFN nanocrystals. Fig. 2 presents a typical TEM image. It shows practically monodisperse particles with an average size about 30.8 – 43.31 nm, which are consistent with the average size obtained from the peak broadening in XRD. Such consistency implies that the LSFN nanoparticles are single crystalline that is favorable to a catalytic application.

Figure 2: TEM image of (a) LFN (b) LSFNO.1 (c) LSFNO.2 (2)



All structural informations and particle sizes obtained with Scherer relation either specific areas of BET technique are collected in Table.1.

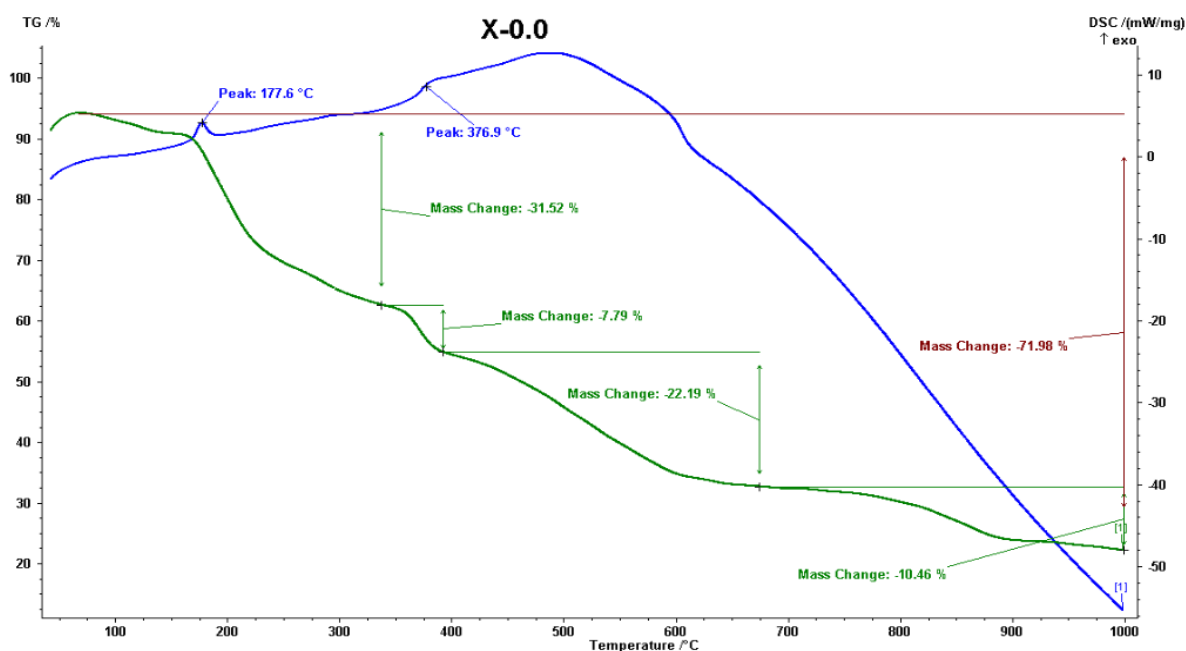
Table 1: Structural informations and BET specific area of LSFNx NPs

Sample	Structure	Space group	Lattice parameters (Å)			Unit cell volume (Å ³)	Cristallite size (nm)	S _{BET} (m ² /g)
			a	b	c			
x = 0.0	Orthorhombic	Pbnm	5.5389	5.5162	7.8130	238.71	43.31	5.6647
x = 0.1	Rhomboedric	R-3C	4.9890	4.9890	17.0620	367.78	31.50	20.6689
x = 0.2	Rhomboedric	R-3C	5.0380	5.0380	13.7720	302.72	30.80	7.6830

Simultaneous DSC-TG

TG and DSC measurements were performed to study the thermal behavior of the sol and the respective curve of the LSFN_{0.0} is shown in Fig. 3. For the sample LaFe_{0.7}Ni_{0.3}O₃, the TG curve shows that the weight loss started at 155 °C, An abrupt weight loss of -31.52% occurs, which ends about at 335 °C.

The DSC curve indicates that an exothermic peak is at about 177.6 °C, which is related to the burning of the sol. Another weight loss of -7.79% occurs accompanied by second exothermic peak at 376.9°C, which is probably due to the combustion of residual carbon. A final exothermic peak is observed at a temperature just above 500 °C although the weight loss of -22.19%, which is due to the formation of LaFe_{0.7}Ni_{0.3}O₃ crystals.

Figure 3: DSC TG curves of LaFe_{0.7}Ni_{0.3}O₃


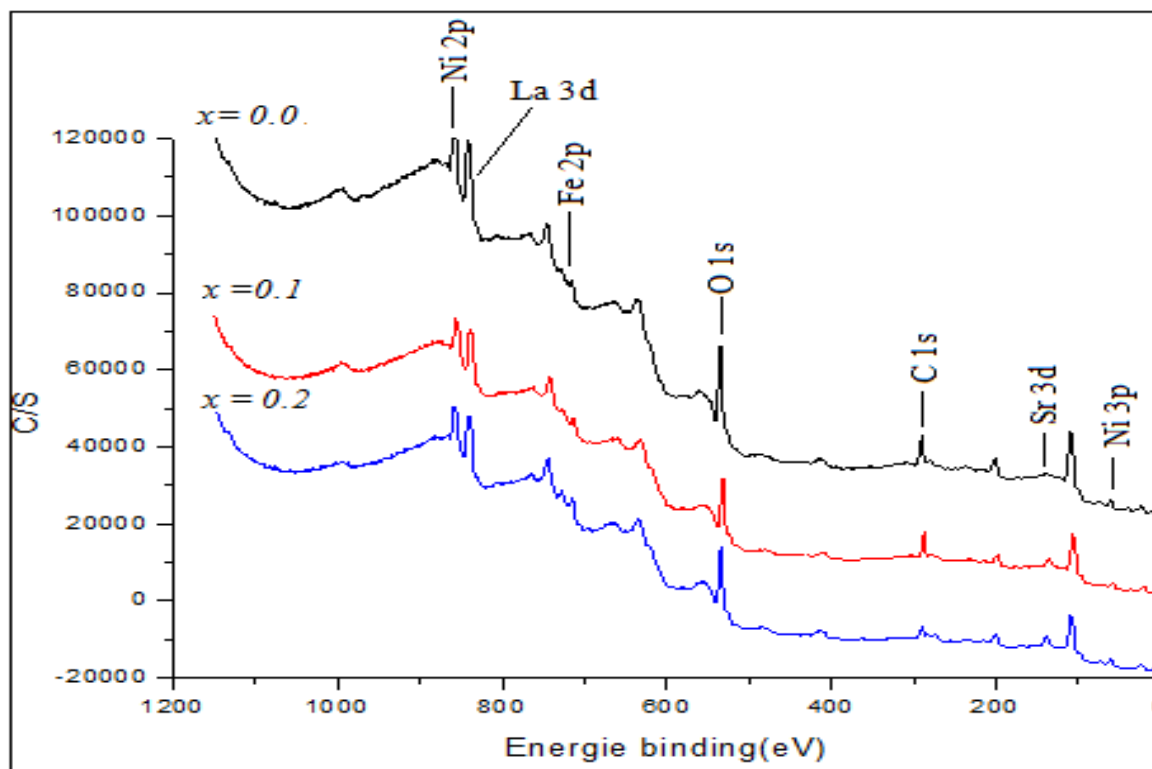
X-ray photoelectron spectroscopy(XPS)

The X-ray photoelectron spectroscopy (XPS) was used to characterize the element chemical state for LSFN_x materials, as shown in Fig. 4. The surface characterization was realized for XPS analysis using C1s as reference. Table. 2 contains binding energies values: O 1s, La 3d, Sr 3d, Fe 2p, Ni 2p and Ni 3p and their atomic concentrations. For all samples LSFN_x ($x = 0.0, 0.1$ and 0.2), La 3d_{5/2} are registered in 842.59, 835.97 and 837.97 eV, La 3d_{3/2} are registered in 859.69, 852.98 and 858.80 eV [26], data indicate that lanthanum is probably present in trivalent form. Strontium presents transition in Sr 3d_{3/2} with bending energies 135.74-138.24 eV may corresponds to SrCO₃, that strontium present bivalent form. B site in this oxide is presented by iron and nickel, that iron bending energies values presents both transition state Fe 2p_{1/2} and Fe 2p_{3/2} with only trivalent oxidation form [27] and very small amount of oxidized ions but nickel presented in two transition states Ni 2p and very small amount of Ni 3p, the peaks of Ni 2p are located in the energy range (856.94-859.50 eV), probably due to Ni(OH)₂, there is a overlapping for La 3d_{3/2} and Ni 2p_{3/2}. The XPS spectra present two O 1s photolines that correspond to two different oxygen species. The lower binding energy, can be associated with lattice, while the higher energy, can be associated with the species of absorbed oxygen, although this latter fraction should also contain adsorbed oxygen. In the literature [26], the binding energy corresponding to the oxygen species appear in 528.3 and 531.9 eV. For the species OH⁻, these values are 529.7 and 532.2 eV, and for metal carbonate are 535.61- 536.23 eV, respectively [28]. The similarity between this binding energies results in that the values presented in this work indicate a higher possibility of this species to exist.

 Table 2: XPS informations of LSFN_x NPs calcined at 700°C

Level	x= 0.0		x = 0.1		x = 0.2	
	E.B (eV)	A.C (%)	E.B (eV)	A.C (%)	E.B (eV)	A.C (%)
O 1s	533.43	38.9	530.81	39.3	533.14	44.9
	536.23		533.28		535.61	
C 1s	289.74	25.8	286.94	27.7	289.20	14.8
La 3d	842.59	10.0	835.97	9.2	837.97	10.4
	859.69		852.98		858.80	
Sr 3d	—	00	135.74	3.4	138.12	4.2
Fe 2p	714.53	< 0.1	712.21	< 0.1	714.20	< 0.1
	734.09		725.93		727.66	
Ni 2p	859.50	25.3	856.94	20.3	858.96	25.7
Ni 3p	72.31	< 0.1	69.54	< 0.1	60.00	< 0.1

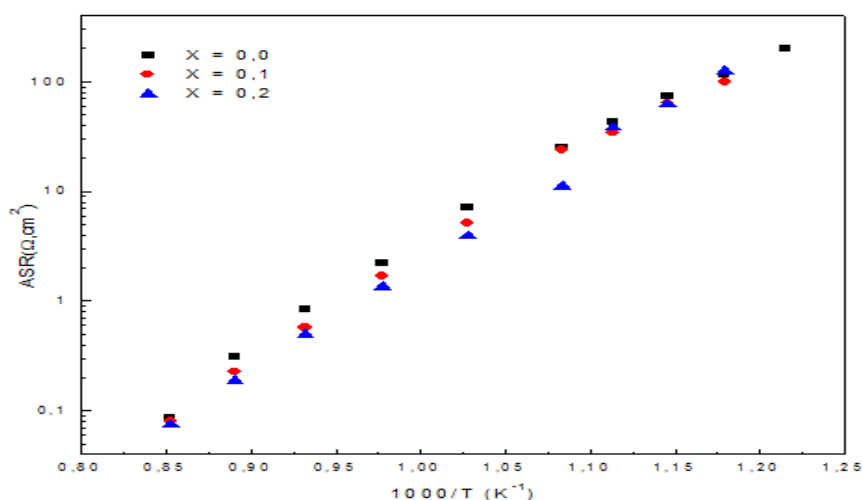
Figure 4: XPS spectra of a survey scan of the LSFNx powders



Atomic concentrations present high values of O1s, C1s, Ni2p, La3d, Sr3d respectively, on the perovskite surface that the active element is the nickel, shift on LSFN_{0.1} energies bending to lower values indicate that there is a reduction to be found for B site elements.

ASR measurements

Figure 5: ASR values for the symmetrical cells under air of LSFN NPs



Symmetrical cells of the different electrodes with LSGM were prepared in order to compare their electrochemical efficiency. The cells were sintered at 1100 °C for 1 h to prevent an excessive reactivity between the materials, considering the previous compatibility study. The area specific polarization resistance (ASR) values were calculated from the overall polarization resistance R_p and electrode surface S by: $ASR = R_p S / 2$, where the factor 2 is due to the symmetrical configuration. The temperature dependence of the area-

specific polarization resistance (ASR) is shown in Fig. 5. By comparison between ASR values it is found that $\text{La}_{0.8}\text{Sr}_{0.2}\text{Fe}_{0.7}\text{Ni}_{0.3}\text{O}_3 < \text{La}_{0.8}\text{Sr}_{0.2}\text{Fe}_{0.7}\text{Ni}_{0.3}\text{O}_3 < \text{LaFe}_{0.7}\text{Ni}_{0.3}\text{O}_3$ in temperature range 650-900°C, it should be commented that the ASR values determined under symmetrical atmosphere are possibly larger than those obtained from fuel cell test, because SOFC operates under an oxygen chemical potential gradient with oxidant and reducing gases in the cathode and anode respectively, and the current across the cell decreases the polarization resistance.

Another issue to be considered is that the efficiency of the double perovskite anode materials seems to depend significantly on the reducing conditions [24] ASR value of LSFN(x = 0.2) at 575°C is higher than LSFN(x = 0.0 and 0.1) and higher than LSFN(x = 0.1) at 625°C, this can be explained by the coexistence of phase in this sample with need high temperature values.

CONCLUSION

In summary, the $\text{La}_{1-x}\text{Sr}_x\text{Fe}_{0.7}\text{Ni}_{0.3}\text{O}_3$, (x = 0.0, 0.1 & 0.2) NPs were successfully prepared by sol-gel combustion method. XRD patterns reveal the perovskite nature of NPs having single phase. Particle sizes are calculated using Scherer formula and checked by TEM images which are in agreement and decrease with doping, specific area is calculated by using BET technique, that, all samples have important values. The active element is Ni having bivalent oxidation state. Electrochemical behavior was observed in all samples, it was found that ASR values decrease with doping and the efficiency of LSFN NPs as symmetrical cell on LSGM electrolyte is investigated with excellent results in high temperature values.

ACKNOWLEDGEMENT

Author is so much grateful for the scientific support of applied physics I, inorganic chemistry department and investigation center, university of Malaga, Spain.

REFERENCES

- [1] Iwasaki K, Ito T, Yoshino M, Matsui T, Nagasaki T and Arita Y. *J Alloys Compounds* 2007; 430: 297.
- [2] Pecchi G, Reyes P, Zamora R, Cadus LE and Fierro JLG. *Solid State Chem* 2008; 131: 905.
- [3] Kharton VV, Viskup AP, Naumovich EN and Tikhonovich VN. *Mater Res Bull* 1999; 34:1311.
- [4] Kuang K, Lee HY and Goodenough J B. *J Electrochem Soc* 1998; 145: 3220.
- [5] Rapagna S, Provendier H, Petit C, Keinnemann A and Foscolo PU. *J Biomass Bioenergy* 2002; 22: 377.
- [6] Provendier H, Petit C, Estournes C, Libs S and Keinnemann A. *Appl. Catal A: General* 1999; 180: 163.
- [7] Mawdsley JR, Krause TR. *Appl Catal* 2008 ; A 334: 311.
- [8] Provendier H, Petit C, Keinnemann A, *Acad CR. Sci. Paris, Série IIc. Chim./Chem* 2001 ; 4: 57.
- [9] Sarma DD, Chainani A. *J Solid State Chem* 1994; 111: 208.
- [10] Choi SO, Moon SH. *Catalysis Today* 2009; 146: 148–153.
- [11] Saad AA, Khan W, Dhiman P, Naqvi AH and Singh M. *Electronic Materials Letters* 2013;9(1):77-81.
- [12] Seyfi B, Baghalha M, and Kazemianb H. *J Chem Eng* 2009; 148: 306 .
- [13] Kemik N, Takamura Y, and Navrotsky A. *J Solid State Chem* 2011; 184: 2118.
- [14] Lee CW, Behera RK, Okamoto S, Devanathan R, Wachsman ED, Phillpot SR, Sinnott SB. *J Am Ceram Soc* 2011; 94: 1931 .
- [15] Berchmansa LJ, Sindhub R, Angappana R and Augustina CO. *J Mater Process Technol* 2008; 207:301.
- [16] Waernhus I, Vullum PE, Holmestad R, Grande T and Wiik K. *Solid State Ion* 2005; 176: 2783.
- [17] Waernhus I, Grande T and Wiik K. *Solid State Ion* 2005; 176: 2609.
- [18] Tsipis EV, Kiselev EA, Kolotygin VA, Waerenborgh JC, Cherepanov VA and Kharton VV. *Solid State Ion* 2008; 179: 2170.
- [19] Chiba R, F. Yoshimura and Y Sakurai. *Solid State Ion* 1999;124:281.
- [20] Gateshki M, Suescun L, Kolesnik S, Mais J, Swierczek K, Short S and Dabrowski BJ. *Solid State Chem* 2008; 181: 1833.
- [21] Swierczek K, Marzec J, Pałubiak D and Zajac W. *Solid State Ion* 2006; 177: 1811.
- [22] Bevilacqua M, Montini T, Tavagnacco C, Vicario G, Fornasiero P and Graziani M. *Solid State Ion* 2006; 177: 2957.
- [23] dos Santos-Gómez L, León-Reina L, Porras-Vázquez JM, Losilla ER and Marrero-López D. *Solid State Ion* 2013; 239: 1–7.



- [24] Oliveira FS, Pimentel PM, Oliveira RMPB, Melo DMA, Melo MAF. Mater Lett 2010; 64: 2700–2703.
- [25] Birks LS and Friedman H J Appl Phys 1946; 17: 687 .
- [26] O’Connell M, Norman AK, Hüttermann CF, Morris MA. Catal Tod 1999; 47:123-132.
- [27] Grosvenor AP, Kobe BA, Biesinger MC and McIntyre NS, Surf. Interface Anal, 2004; 36: 1564–1574.
- [28] Nohira H, Tsai W, Besling W, Young E, Petry J, Conard T, Vandervorst W, De Gendt S, Heyns M, Maes J and Tuominen M. J Non-Crystall Solids 2002; 303: 83–87.